

DYNNLO

A fully exclusive parton level Monte Carlo code
for the Drell-Yan process in NNLO QCD

Milan University & INFN, Milan



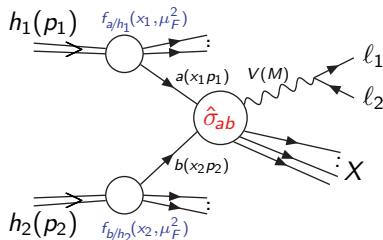
In collaboration with: S. Catani, L. Cieri, D. de Florian & M. Grazzini

Saha Theory Workshop – SINP – Kolkata – 26/2/2016

The Drell-Yan process

$$h_1(p_1) + h_2(p_2) \rightarrow V(M) + X \rightarrow \ell_1 + \ell_2 + X$$

where $V = \gamma^*, Z^0, W^\pm$ and $\ell_1 \ell_2 = \ell^+ \ell^-, \ell \nu_\ell$



According to the QCD factorization theorem:

$$d\sigma(p_1, p_2, \{y\}) = \sum_{a,b} \int_0^1 dx_1 \int_0^1 dx_2 f_{a/h_1}(x_1, \mu_F^2) f_{b/h_2}(x_2, \mu_F^2) d\hat{\sigma}_{ab}(x_1 p_1, x_2 p_2, \{y\}; \mu_F^2) + \mathcal{O}\left(\frac{\Lambda^2}{M^2}\right).$$

$$d\hat{\sigma}_{ab}(\hat{p}_1, \hat{p}_2, \{y\}; \mu_F^2) = d\hat{\sigma}_{ab}^{(0)}(\hat{p}_1, \hat{p}_2, \{y\}; \mu_F^2) + \alpha_S(\mu_R^2) d\hat{\sigma}_{ab}^{(1)}(\hat{p}_1, \hat{p}_2, \{y\}; \mu_F^2) \\ + \alpha_S^2(\mu_R^2) d\hat{\sigma}_{ab}^{(2)}(\hat{p}_1, \hat{p}_2, \{y\}; \mu_F^2, \mu_R^2) + \mathcal{O}(\alpha_S^3).$$

$\{y\} \equiv$ Infrared safe constraints on final states.

The NNLO q_T subtraction formalism

- A NNLO extension of the subtraction formalism valid for the production of **colourless high-mass system** in hadron collisions was proposed by [Catani, Grazzini('07)] and applied for Higgs boson production in the parton level Monte Carlo code **HNNLO**.
- This method was used to perform a fully exclusive NNLO calculation for vector boson production which includes the γ - Z interference, finite-width effects, the leptonic decay of the vector bosons and the corresponding spin correlations [Catani, Cieri, G.F., de Florian, Grazzini('09)].
An analogous computation exists [Melnikov, Petriello('06)].
- The calculation is implemented in a parton level Monte Carlo code **DYNNLO**.

The code DYNULO

- The Fortran code of **DYNULO** can be downloaded from:
<http://theory.fi.infn.it/grazzini/dy.html>
- It has been tested on Linux and OSX Systems.
- Extract the main directory `dynulo/`:

```
$ tar xzvf dynulo-v1.5.tgz
```
- Compile the code:

```
$ cd dynulo/  
$ make
```
- Run the executable:

```
$ cd bin/  
$ ./dynulo < infile
```

The structure of the main directory:

- `$dynnlo/bin/` The working directory.
- `$dynnlo/doc/` The directory containing a note.
- `$dynnlo/obj/` The directory containing the object files.
- `$dynnlo/src/` The directory containing the source files.

The structure of the working directory:

- `$dynnlo/bin/dynnlo` The executable file.
- `$dynnlo/bin/infile` The input file.
- `$dynnlo/bin/Pdfdata` The directory containing the PDFs grids.

The input file

This is a typical example of input file:

```
8d3 !  sroot  Double precision variable for CM energy (GeV).
1 1 !  ih1 ih2  Integers identifying the beam: (anti)proton=(-)1.
3 !  nproc  Vector boson produced:  $W^+ \rightarrow l^+\nu$  (1),  $W^- \rightarrow l^-\bar{\nu}$  (2),  $Z/\gamma^* \rightarrow l^+l^-$  (3).
91.1876d0 91.1876d0 !  mur, muf  Renorm. and factoriz. scales (GeV).
2 !  order  Order of calculation LO (0), NLO (1), NNLO (2).
'tota' !  part  String identifying the part of the calculation performed:
                real (real), virtual (virt), total (tota)
.false. !  zerowidth  If true the zero width approximation for boson is used.
66d0 116d0 !  mwmin, mwmax  Limits on the vector boson (lepton pair) invariant mass.
15 1000000 !  itmx1, ncall1  # of iterations and calls to the Vegas grid.
30 8000000 !  itmx2, ncall2  # of iterations and calls to the Vegas run.
617 !  rseed  Random number seed.
92 0 !  iset nset  Integers for PDFs set and error member (native interface).
'MSTW2008nnlo68cl.LHgrid' 0 !  set, member (LHAPDFs) String and integer for
                PDFs set and error member (LHAPDF interface).
'nnlo' !  runstring  String for grid and output files.
```

Infrared cuts on final states

Infrared cuts on final states can be set in the `src/User/cuts.f` file.
For instance:

```
pt3=dsqrt(pjet(3,1)**2+pjet(3,2)**2)
pt4=dsqrt(pjet(4,1)**2+pjet(4,2)**2)
eta3=etarap(3,pjet)
eta4=etarap(4,pjet)
```

C Cuts in GeV

```
if(pt3.lt.25d0) cuts=.true.
if(pt4.lt.25d0) cuts=.true.
if(dabs(eta3).gt.1d0) cuts=.true.
if(dabs(eta4).gt.1d0) cuts=.true.
```

Input parameters and setup file

In the calculation we use the so called G_μ scheme (G_F, m_Z, m_W).

The values of input parameters are:

$G_F = 1.1663787 \times 10^{-5} \text{ GeV}^{-2}$ $m_W = 80.385 \text{ GeV}$, $\Gamma_W = 2.085 \text{ GeV}$,
 $m_Z = 91.1876 \text{ GeV}$, $\Gamma_Z = 2.4952 \text{ GeV}$, $V_{ud} = 0.97427$, $V_{us} = 0.2253$,
 $V_{ub} = 0.00351$, $V_{cd} = 0.2252$, $V_{cs} = 0.97344$, $V_{cb} = 0.0412$ ([PDG ('12)]).

Important features can be set in the `src/Need/setup.f` file:

CC Narrow width approximation

```
zerowidth=.false.
```

CC Branching ratio

```
removebr=.false.
```

CC Lepton isolation is set in `src/User/isolation.f`

```
isol=.true.
```

CC Jets are reconstructed according to the k_T algorithm

CC Parameters used to define jets

```
ptjetmin=0d0
```

```
etajetmin=0d0
```

```
etajetmax=20d0
```

```
Rcut=0.4d0
```


Plotted distributions

Desired distributions in the form of bin histograms can be set in the `src/User/plotter.f` file.

A Topdrawer file will be generated.

Let's consider for instance Z production at the Tevatron:

```
eta3=etarap(3,p)
```

```
pt3=pt(3,p)
```

```
y34=yraptwo(3,4,p)
```

```
pt34=pttwo(3,4,p)
```

```
CC
```

```
n=1
```

```
call bookplot(n,tag,'eta3',eta3,wt,-4d0,4d0,0.1d0,'lin')
```

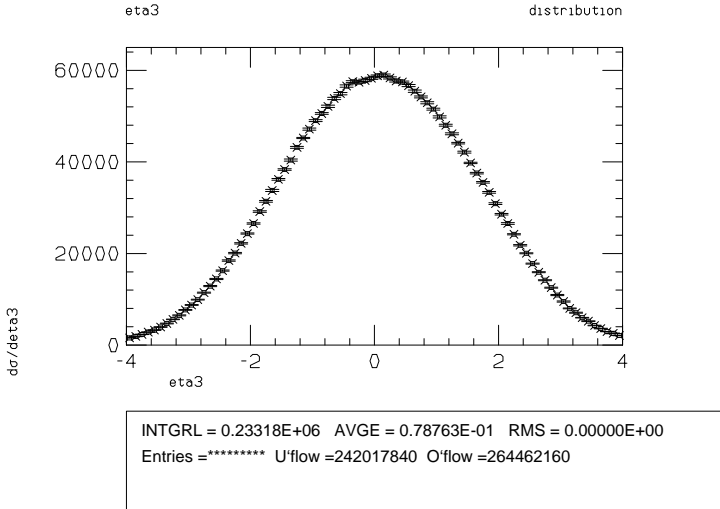
```
n=n+1
```

```
call bookplot(n,tag,'y34',y34,wt,-3d0,3d0,0.25d0,'lin')
```

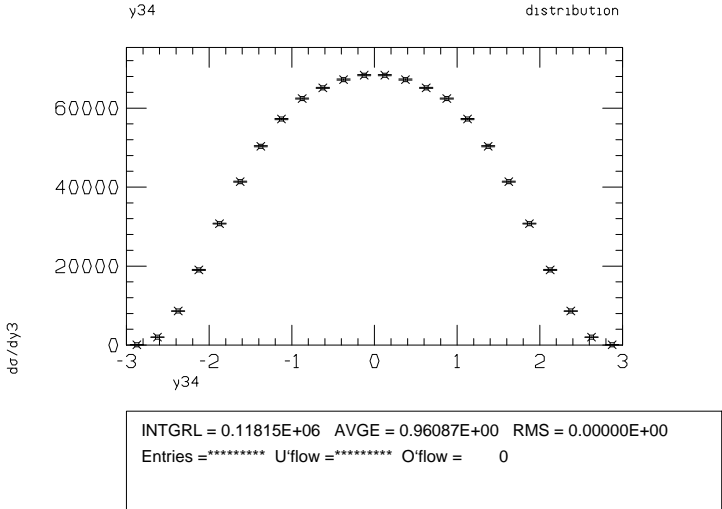
```
n=n+1
```

```
call bookplot(n,tag,'pt34',pt34,wt,0d0,100d0,2d0,'log')
```

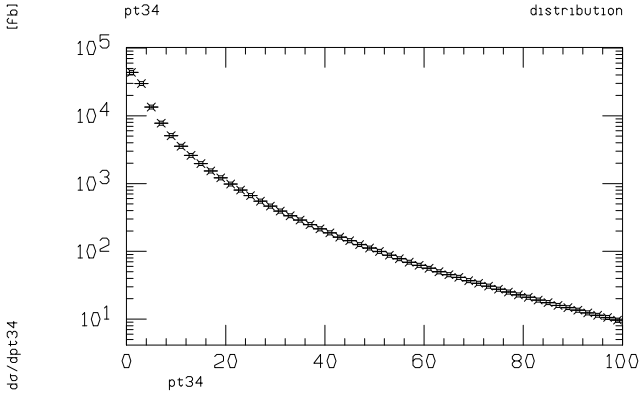
```
n=n+1
```



Z production at the Tevatron: electron rapidity distribution.



Z production at the Tevatron: Z rapidity distribution.

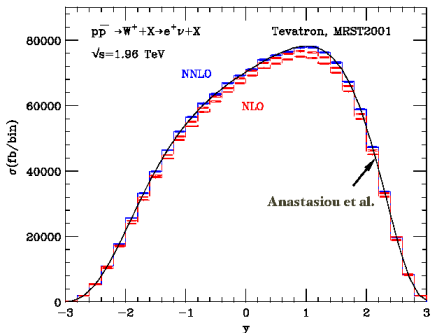


INTGRL = 0.23466E+06 AVGE = 0.57931E+01 RMS = 0.00000E+00
 Entries = 152189516 U'flow = 0 O'flow = 409990100

Z production at the Tevatron: Z transverse momentum distribution.

Numerical Results

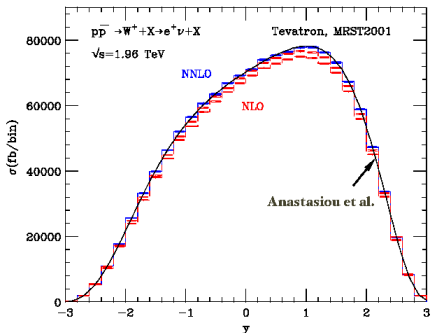
Rapidity distribution



Rapidity distribution for W^+ production at the Tevatron (no cuts).

- No cuts are applied on final states.
- The error bars in the histograms refer to the Monte Carlo numerical errors.
- NNLO result compared with the NLO band (obtained by varying $m_Z/2 \leq \mu_F = \mu_R \leq 2 m_Z$) and with the NNLO analytical result by [Anastasiou et al. ('03)].
- Results from DYNNLO MC code agree with known analytical results within the numerical error.

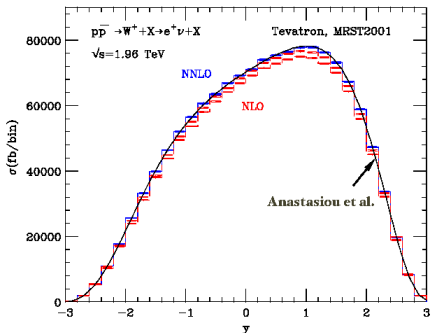
Rapidity distribution



Rapidity distribution for W^+ production at the Tevatron (no cuts).

- No cuts are applied on final states.
- The error bars in the histograms refer to the Monte Carlo numerical errors.
- NNLO result compared with the NLO band (obtained by varying $m_Z/2 \leq \mu_F = \mu_R \leq 2 m_Z$) and with the NNLO analytical result by [Anastasiou et al. ('03)].
- Results from DYNNLO MC code agree with known analytical results within the numerical error.

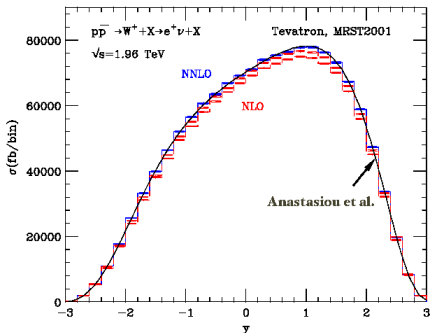
Rapidity distribution



Rapidity distribution for W^+ production at the Tevatron (no cuts).

- No cuts are applied on final states.
- The error bars in the histograms refer to the Monte Carlo numerical errors.
- NNLO result compared with the NLO band (obtained by varying $m_Z/2 \leq \mu_F = \mu_R \leq 2 m_Z$) and with the NNLO analytical result by [Anastasiou et al. ('03)].
- Results from DYNNLO MC code agree with known analytical results within the numerical error.

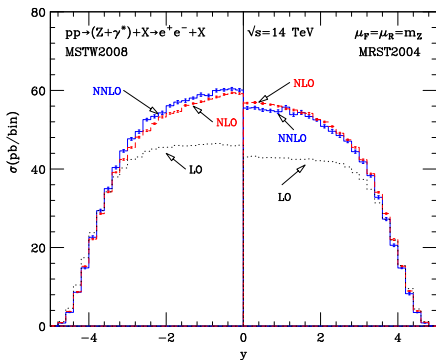
Rapidity distribution



- No cuts are applied on final states.
- The error bars in the histograms refer to the Monte Carlo numerical errors.
- NNLO result compared with the NLO band (obtained by varying $m_Z/2 \leq \mu_F = \mu_R \leq 2 m_Z$) and with the NNLO analytical result by [Anastasiou et al. ('03)].
- Results from DYNNLO MC code agree with known analytical results within the numerical error.

Rapidity distribution for W^+ production at the Tevatron (no cuts).

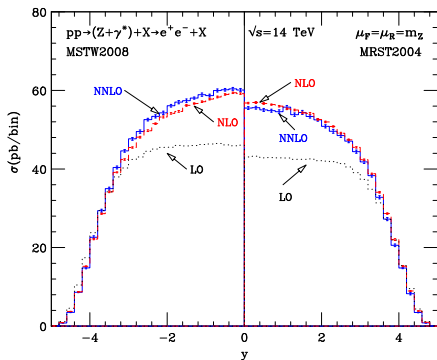
Rapidity distribution



Rapidity distribution for Z production at the LHC (no cuts).

- No cuts are applied on final states.
- The error bars in the histograms refer to the Monte Carlo numerical errors.
- Left panel: MSTW 2008 PDFs:
 $\sigma_{NLO} = 2.030 \pm 0.001 \text{ nb}$,
 $\sigma_{NNLO} = 2.089 \pm 0.003 \text{ nb}$.
- Right panel: MRST 2004 PDFs:
 $\sigma_{NLO} = 1.992 \pm 0.001 \text{ nb}$,
 $\sigma_{NNLO} = 1.954 \pm 0.003 \text{ nb}$.
- σ_{NNLO} scale variations:
-1.7% for $\mu_R = \mu_F = m_Z/2$,
+1.5% for $\mu_R = \mu_F = 2 m_Z$.
- Typical computing time for smooth distributions with a percent level accuracy on a standard PC:
LO: few minutes, NLO: few hours, NNLO: three days.
The computing time for cross sections is reduced by a factor two.

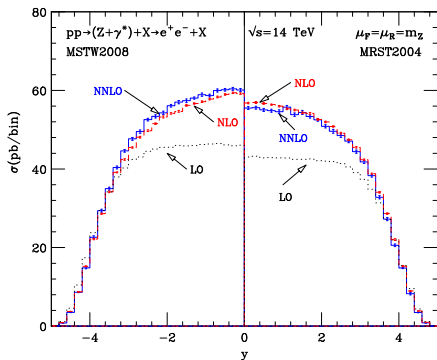
Rapidity distribution



Rapidity distribution for Z production at the LHC (no cuts).

- No cuts are applied on final states.
- The error bars in the histograms refer to the Monte Carlo numerical errors.
- Left panel: MSTW 2008 PDFs:
 $\sigma_{NLO} = 2.030 \pm 0.001$ nb,
 $\sigma_{NNLO} = 2.089 \pm 0.003$ nb.
- Right panel: MRST 2004 PDFs:
 $\sigma_{NLO} = 1.992 \pm 0.001$ nb,
 $\sigma_{NNLO} = 1.954 \pm 0.003$ nb.
- σ_{NNLO} scale variations:
-1.7% for $\mu_R = \mu_F = m_Z/2$,
+1.5% for $\mu_R = \mu_F = 2 m_Z$.
- Typical computing time for smooth distributions with a percent level accuracy on a standard PC:
LO: few minutes, NLO: few hours, NNLO: three days.
The computing time for cross sections is reduced by a factor two.

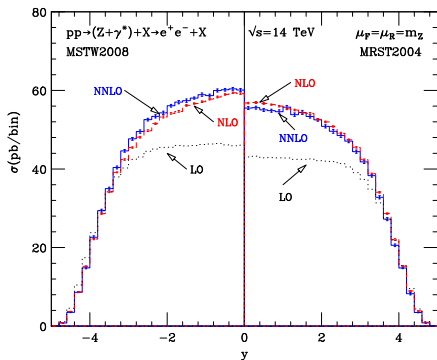
Rapidity distribution



Rapidity distribution for Z production at the LHC (no cuts).

- No cuts are applied on final states.
- The error bars in the histograms refer to the Monte Carlo numerical errors.
- Left panel: MSTW 2008 PDFs:
 $\sigma_{NLO} = 2.030 \pm 0.001$ nb,
 $\sigma_{NNLO} = 2.089 \pm 0.003$ nb.
- Right panel: MRST 2004 PDFs:
 $\sigma_{NLO} = 1.992 \pm 0.001$ nb,
 $\sigma_{NNLO} = 1.954 \pm 0.003$ nb.
- σ_{NNLO} scale variations:
-1.7% for $\mu_R = \mu_F = m_Z/2$,
+1.5% for $\mu_R = \mu_F = 2 m_Z$.
- Typical computing time for smooth distributions with a percent level accuracy on a standard PC:
LO: few minutes, NLO: few hours, NNLO: three days.
The computing time for cross sections is reduced by a factor two.

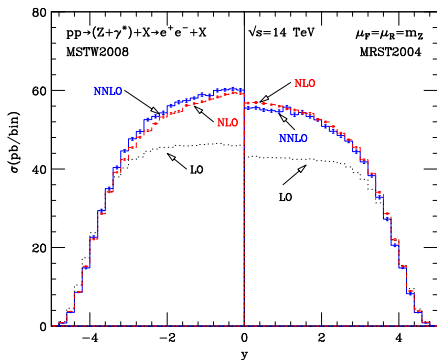
Rapidity distribution



Rapidity distribution for Z production at the LHC (no cuts).

- No cuts are applied on final states.
- The error bars in the histograms refer to the Monte Carlo numerical errors.
- Left panel: MSTW 2008 PDFs:
 $\sigma_{NLO} = 2.030 \pm 0.001$ nb,
 $\sigma_{NNLO} = 2.089 \pm 0.003$ nb.
- Right panel: MRST 2004 PDFs:
 $\sigma_{NLO} = 1.992 \pm 0.001$ nb,
 $\sigma_{NNLO} = 1.954 \pm 0.003$ nb.
- σ_{NNLO} scale variations:
-1.7% for $\mu_R = \mu_F = m_Z/2$,
+1.5% for $\mu_R = \mu_F = 2 m_Z$.
- Typical computing time for smooth distributions with a percent level accuracy on a standard PC:
LO: few minutes, NLO: few hours, NNLO: three days.
The computing time for cross sections is reduced by a factor two.

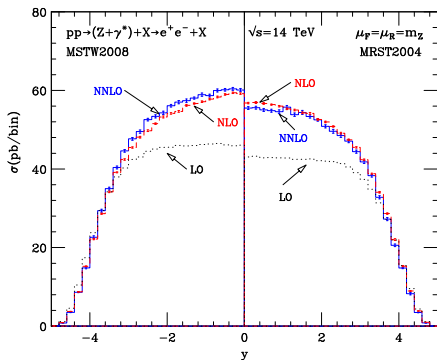
Rapidity distribution



Rapidity distribution for Z production at the LHC (no cuts).

- No cuts are applied on final states.
- The error bars in the histograms refer to the Monte Carlo numerical errors.
- Left panel: MSTW 2008 PDFs:
 $\sigma_{NLO} = 2.030 \pm 0.001$ nb,
 $\sigma_{NNLO} = 2.089 \pm 0.003$ nb.
- Right panel: MRST 2004 PDFs:
 $\sigma_{NLO} = 1.992 \pm 0.001$ nb,
 $\sigma_{NNLO} = 1.954 \pm 0.003$ nb.
- σ_{NNLO} scale variations:
-1.7% for $\mu_R = \mu_F = m_Z/2$,
+1.5% for $\mu_R = \mu_F = 2 m_Z$.
- Typical computing time for smooth distributions with a percent level accuracy on a standard PC:
LO: few minutes, NLO: few hours, NNLO: three days.
The computing time for cross sections is reduced by a factor two.

Rapidity distribution



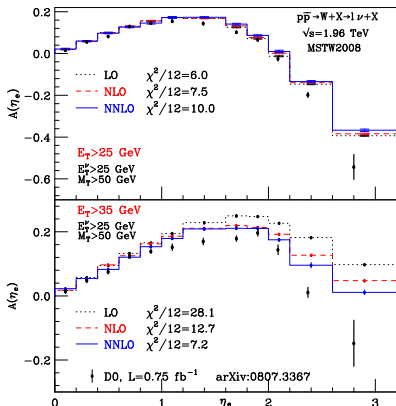
Rapidity distribution for Z production at the LHC (no cuts).

- No cuts are applied on final states.
- The error bars in the histograms refer to the Monte Carlo numerical errors.
- Left panel: MSTW 2008 PDFs:
 $\sigma_{NLO} = 2.030 \pm 0.001 \text{ nb}$,
 $\sigma_{NNLO} = 2.089 \pm 0.003 \text{ nb}$.
- Right panel: MRST 2004 PDFs:
 $\sigma_{NLO} = 1.992 \pm 0.001 \text{ nb}$,
 $\sigma_{NNLO} = 1.954 \pm 0.003 \text{ nb}$.
- σ_{NNLO} scale variations:
-1.7% for $\mu_R = \mu_F = m_Z/2$,
+1.5% for $\mu_R = \mu_F = 2 m_Z$.
- Typical computing time for smooth distributions with a percent level accuracy on a standard PC:
LO: few minutes, NLO: few hours, NNLO: three days.
The computing time for cross sections is reduced by a factor two.

Lepton charge asymmetry:

$$A(y_l) = \frac{d\sigma(l^+)/dy_l - d\sigma(l^-)/dy_l}{d\sigma(l^+)/dy_l + d\sigma(l^-)/dy_l}$$

- D0 data on electron charge asymmetry [arXiv:0807.3367].
- Selection cuts on final states:
 $E_T^\nu > 25 \text{ GeV}$, $M_T > 50 \text{ GeV}$, $E_T > 25 \text{ GeV}$ (top) and $E_T > 35 \text{ GeV}$ (bottom).
- Lepton isolation requirements:
 $E_T^{\text{iso}}/E_T < 0.15$. Where E_T^{iso} is the hadronic (partonic) transverse energy in a cone along the direction of the lepton momentum with radius $R = 0.4$ in the lepton $(\eta-\phi)$ space
- NNLO corrections can be larger than experimental errors while NNLO scale dependence ($M_W/2 \leq \mu_F = \mu_R \leq 2M_W$) comparable to the Monte Carlo numerical error.
- Inclusion of PDFs errors improves the consistency between data and theory but PDFs errors from different sets do not completely overlap.

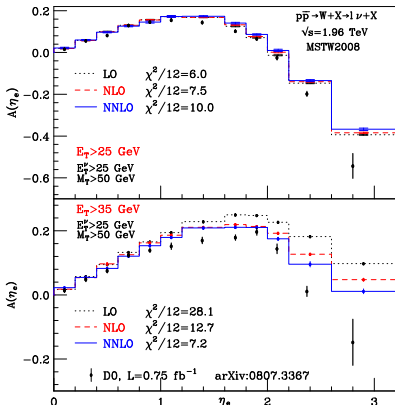


The electron charge asymmetry in LO, NLO and NNLO QCD with MSTW08 PDFs at wide (top) and high (bottom) E_T , compared with D0 data.

Lepton charge asymmetry:

$$A(y_l) = \frac{d\sigma(l^+)/dy_l - d\sigma(l^-)/dy_l}{d\sigma(l^+)/dy_l + d\sigma(l^-)/dy_l}$$

- D0 data on electron charge asymmetry [arXiv:0807.3367].
- Selection cuts on final states: $E_T^\nu > 25$ GeV, $M_T > 50$ GeV, $E_T > 25$ GeV (top) and $E_T > 35$ GeV (bottom).
- Lepton isolation requirements: $E_T^{\text{iso}}/E_T < 0.15$. Where E_T^{iso} is the hadronic (partonic) transverse energy in a cone along the direction of the lepton momentum with radius $R = 0.4$ in the lepton $(\eta-\phi)$ space
- NNLO corrections can be larger than experimental errors while NNLO scale dependence ($M_W/2 \leq \mu_F = \mu_R \leq 2M_W$) comparable to the Monte Carlo numerical error.
- Inclusion of PDFs errors improves the consistency between data and theory but PDFs errors from different sets do not completely overlap.

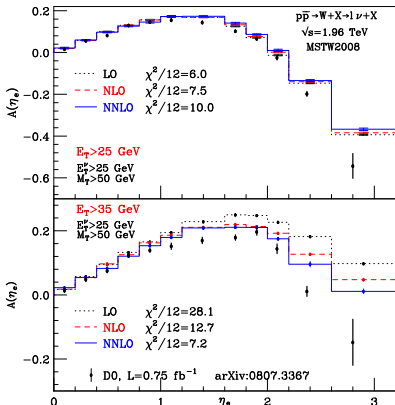


The electron charge asymmetry in LO, NLO and NNLO QCD with MSTW08 PDFs at wide (top) and high (bottom) E_T , compared with D0 data.

Lepton charge asymmetry:

$$A(y_l) = \frac{d\sigma(l^+)/dy_l - d\sigma(l^-)/dy_l}{d\sigma(l^+)/dy_l + d\sigma(l^-)/dy_l}$$

- D0 data on electron charge asymmetry [arXiv:0807.3367].
- Selection cuts on final states: $E_T^\nu > 25 \text{ GeV}$, $M_T > 50 \text{ GeV}$, $E_T > 25 \text{ GeV}$ (top) and $E_T > 35 \text{ GeV}$ (bottom).
- Lepton isolation requirements: $E_T^{\text{iso}}/E_T < 0.15$. Where E_T^{iso} is the hadronic (partonic) transverse energy in a cone along the direction of the lepton momentum with radius $R = 0.4$ in the lepton $(\eta-\phi)$ space
- NNLO corrections can be larger than experimental errors while NNLO scale dependence ($M_W/2 \leq \mu_F = \mu_R \leq 2M_W$) comparable to the Monte Carlo numerical error.
- Inclusion of PDFs errors improves the consistency between data and theory but PDFs errors from different sets do not completely overlap.

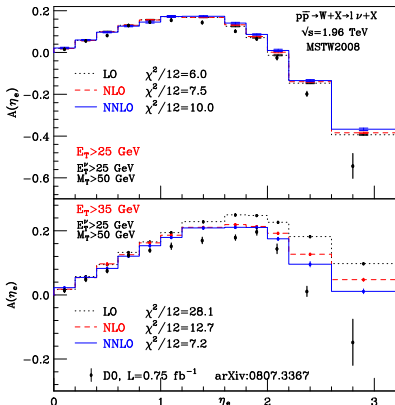


The electron charge asymmetry in LO, NLO and NNLO QCD with MSTW08 PDFs at wide (top) and high (bottom) E_T , compared with D0 data.

Lepton charge asymmetry:

$$A(y_l) = \frac{d\sigma(l^+)/dy_l - d\sigma(l^-)/dy_l}{d\sigma(l^+)/dy_l + d\sigma(l^-)/dy_l}$$

- D0 data on electron charge asymmetry [[arXiv:0807.3367](https://arxiv.org/abs/0807.3367)].
- Selection cuts on final states:
 $E_T^\nu > 25 \text{ GeV}$, $M_T > 50 \text{ GeV}$, $E_T > 25 \text{ GeV}$ (top) and $E_T > 35 \text{ GeV}$ (bottom).
- Lepton isolation requirements:
 $E_T^{\text{iso}}/E_T < 0.15$. Where E_T^{iso} is the hadronic (partonic) transverse energy in a cone along the direction of the lepton momentum with radius $R = 0.4$ in the lepton $(\eta-\phi)$ space
- NNLO corrections can be larger than experimental errors while NNLO scale dependence ($M_W/2 \leq \mu_F = \mu_R \leq 2M_W$) comparable to the Monte Carlo numerical error.
- Inclusion of PDFs errors improves the consistency between data and theory but PDFs errors from different sets do not completely overlap.

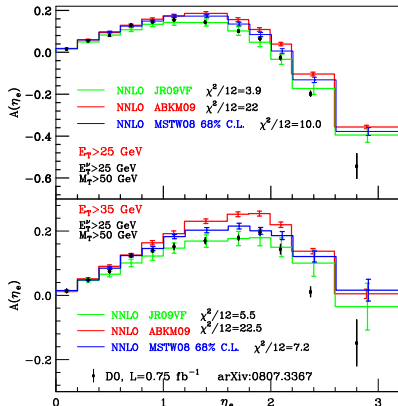


The electron charge asymmetry in LO, NLO and NNLO QCD with MSTW08 PDFs at wide (top) and high (bottom) E_T , compared with D0 data.

Lepton charge asymmetry:

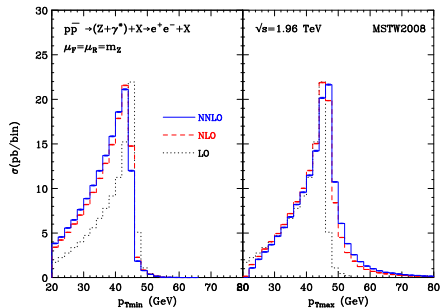
$$A(y_l) = \frac{d\sigma(l^+)/dy_l - d\sigma(l^-)/dy_l}{d\sigma(l^+)/dy_l + d\sigma(l^-)/dy_l}$$

- D0 data on electron charge asymmetry [arXiv:0807.3367].
- Selection cuts on final states: $E_T^\nu > 25 \text{ GeV}$, $M_T > 50 \text{ GeV}$, $E_T > 25 \text{ GeV}$ (top) and $E_T > 35 \text{ GeV}$ (bottom).
- Lepton isolation requirements: $E_T^{\text{iso}}/E_T < 0.15$. Where E_T^{iso} is the hadronic (partonic) transverse energy in a cone along the direction of the lepton momentum with radius $R = 0.4$ in the lepton $(\eta-\phi)$ space
- NNLO corrections can be larger than experimental errors while NNLO scale dependence ($M_W/2 \leq \mu_F = \mu_R \leq 2M_W$) comparable to the Monte Carlo numerical error.
- Inclusion of PDFs errors improves the consistency between data and theory but PDFs errors from different sets do not completely overlap.



The electron charge asymmetry in NNLO QCD with **MSTW08**, **ABKM09**, **JR09VF** PDFs (with errors) at wide (top) and high (bottom) E_T , compared with D0 data.

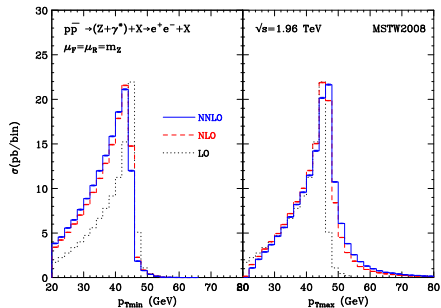
Minimum and maximum p_T distribution



Minimum (left) and maximum (right) lepton p_T distribution for Z production at the Tevatron.

- Cuts: $p_{T\min} \geq 20 \text{ GeV}$; $|\eta| < 2$;
 $70 \text{ GeV} \leq m_{e^+e^-} \leq 110 \text{ GeV}$
- At LO the distributions are kinematically bounded by $p_T < (m_{e^+e^-})_{\max}/2 = 55 \text{ GeV}$
- The NNLO corrections make the $p_{T\min}$ distribution softer, and the $p_{T\max}$ distribution harder.
- Accepted cross sections (errors refer to Monte Carlo numerical errors):
 $\sigma_{LO} = 103.37 \pm 0.04 \text{ pb}$,
 $\sigma_{NLO} = 140.43 \pm 0.07 \text{ pb}$,
 $\sigma_{NNLO} = 143.86 \pm 0.12 \text{ pb}$.
- σ_{NNLO} scales variation:
 -0.6% for $\mu_R = \mu_F = m_Z/2$,
 $+0.3\%$ for $\mu_R = \mu_F = 2 m_Z$.

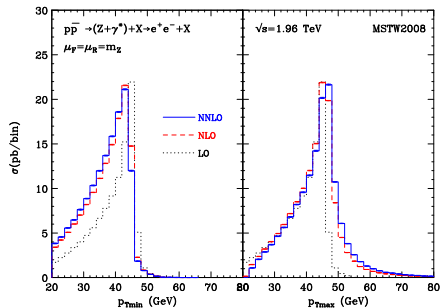
Minimum and maximum p_T distribution



Minimum (left) and maximum (right) lepton p_T distribution for Z production at the Tevatron.

- Cuts: $p_{T\min} \geq 20 \text{ GeV}$; $|\eta| < 2$;
 $70 \text{ GeV} \leq m_{e^+e^-} \leq 110 \text{ GeV}$
- At LO the distributions are kinematically bounded by $p_T < (m_{e^+e^-})_{\max}/2 = 55 \text{ GeV}$
- The NNLO corrections make the $p_{T\min}$ distribution softer, and the $p_{T\max}$ distribution harder.
- Accepted cross sections (errors refer to Monte Carlo numerical errors):
 $\sigma_{LO} = 103.37 \pm 0.04 \text{ pb}$,
 $\sigma_{NLO} = 140.43 \pm 0.07 \text{ pb}$,
 $\sigma_{NNLO} = 143.86 \pm 0.12 \text{ pb}$.
- σ_{NNLO} scales variation:
 -0.6% for $\mu_R = \mu_F = m_Z/2$,
 $+0.3\%$ for $\mu_R = \mu_F = 2 m_Z$.

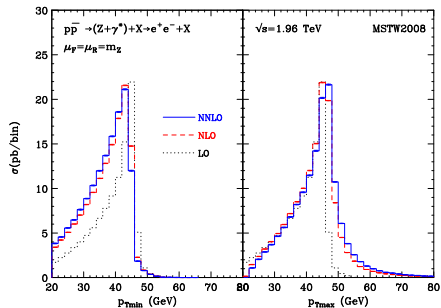
Minimum and maximum p_T distribution



Minimum (left) and maximum (right) lepton p_T distribution for Z production at the Tevatron.

- Cuts: $p_{T\min} \geq 20 \text{ GeV}$; $|\eta| < 2$;
 $70 \text{ GeV} \leq m_{e^+e^-} \leq 110 \text{ GeV}$
- At LO the distributions are kinematically bounded by $p_T < (m_{e^+e^-})_{\max}/2 = 55 \text{ GeV}$
- The NNLO corrections make the $p_{T\min}$ distribution softer, and the $p_{T\max}$ distribution harder.
- Accepted cross sections (errors refer to Monte Carlo numerical errors):
 $\sigma_{LO} = 103.37 \pm 0.04 \text{ pb}$,
 $\sigma_{NLO} = 140.43 \pm 0.07 \text{ pb}$,
 $\sigma_{NNLO} = 143.86 \pm 0.12 \text{ pb}$.
- σ_{NNLO} scales variation:
 -0.6% for $\mu_R = \mu_F = m_Z/2$,
 $+0.3\%$ for $\mu_R = \mu_F = 2 m_Z$.

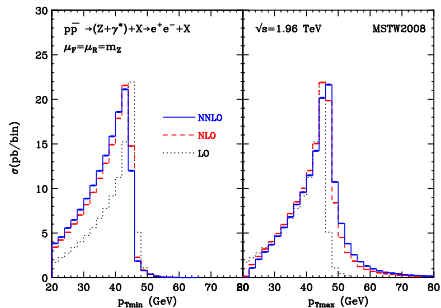
Minimum and maximum p_T distribution



Minimum (left) and maximum (right) lepton p_T distribution for Z production at the Tevatron.

- Cuts: $p_{T\min} \geq 20 \text{ GeV}$; $|\eta| < 2$;
 $70 \text{ GeV} \leq m_{e^+e^-} \leq 110 \text{ GeV}$
- At LO the distributions are kinematically bounded by $p_T < (m_{e^+e^-})_{\max}/2 = 55 \text{ GeV}$
- The NNLO corrections make the $p_{T\min}$ distribution softer, and the $p_{T\max}$ distribution harder.
- Accepted cross sections (errors refer to Monte Carlo numerical errors):
 $\sigma_{LO} = 103.37 \pm 0.04 \text{ pb}$,
 $\sigma_{NLO} = 140.43 \pm 0.07 \text{ pb}$,
 $\sigma_{NNLO} = 143.86 \pm 0.12 \text{ pb}$.
- σ_{NNLO} scales variation:
 -0.6% for $\mu_R = \mu_F = m_Z/2$,
 $+0.3\%$ for $\mu_R = \mu_F = 2 m_Z$.

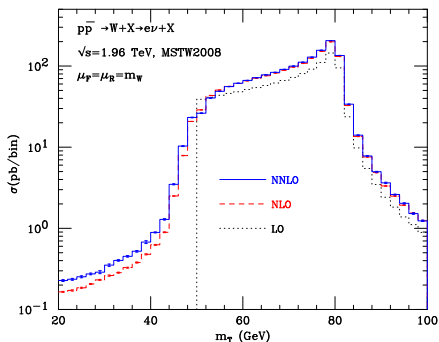
Minimum and maximum p_T distribution



Minimum (left) and maximum (right) lepton p_T distribution for Z production at the Tevatron.

- Cuts: $p_{T\min} \geq 20 \text{ GeV}$; $|\eta| < 2$;
 $70 \text{ GeV} \leq m_{e^+e^-} \leq 110 \text{ GeV}$
- At LO the distributions are kinematically bounded by $p_T < (m_{e^+e^-})_{\max}/2 = 55 \text{ GeV}$
- The NNLO corrections make the $p_{T\min}$ distribution softer, and the $p_{T\max}$ distribution harder.
- Accepted cross sections (errors refer to Monte Carlo numerical errors):
 $\sigma_{LO} = 103.37 \pm 0.04 \text{ pb}$,
 $\sigma_{NLO} = 140.43 \pm 0.07 \text{ pb}$,
 $\sigma_{NNLO} = 143.86 \pm 0.12 \text{ pb}$.
- σ_{NNLO} scales variation:
 -0.6% for $\mu_R = \mu_F = m_Z/2$,
 $+0.3\%$ for $\mu_R = \mu_F = 2 m_Z$.

Transverse mass distribution

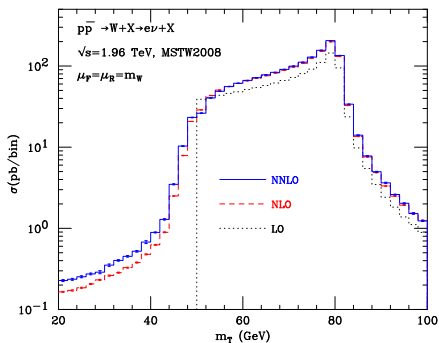


Transverse mass distribution for W production at the Tevatron:

$$m_T = \sqrt{2p_T^l p_T^{\text{miss}} (1 - \cos \phi_{l\nu})}$$

- Cuts: $p_T^{\text{miss}} \geq 25 \text{ GeV}$; $|\eta| < 2$; $p_T^l \geq 20 \text{ GeV}$
- LO distribution bounded at $m_T = 50 \text{ GeV}$. Around the bound there are perturbative instabilities from LO to NLO and to NNLO (Sudakov shoulder [Catani, Webber('97)]).
- Below the boundary, the $\mathcal{O}(\alpha_S^2)$ corrections are large (e.g. +40% at $m_T \sim 30 \text{ GeV}$). Not unexpected: in this region the $\mathcal{O}(\alpha_S^2)$ result is only a NLO calculation.
- Accepted cross sections (errors refer to Monte Carlo numerical errors):
 $\sigma_{LO} = 1.61 \pm 0.001 \text{ nb}$
 $\sigma_{NLO} = 1.550 \pm 0.001 \text{ nb}$
 $\sigma_{NNLO} = 1.586 \pm 0.002 \text{ nb}$
- σ_{NNLO} scales variation:
 -0.8% for $\mu_R = \mu_F = m_W/2$,
 $+0.6\%$ for $\mu_R = \mu_F = 2 m_W$.

Transverse mass distribution

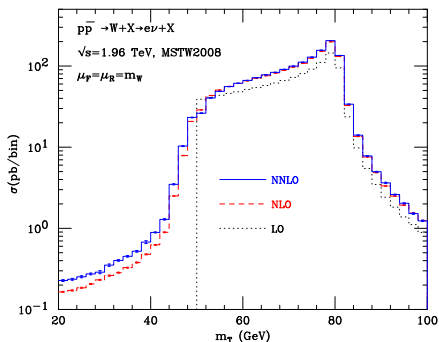


Transverse mass distribution for W production at the Tevatron:

$$m_T = \sqrt{2p_T^l p_T^{miss} (1 - \cos \phi_{l\nu})}$$

- Cuts: $p_T^{miss} \geq 25 \text{ GeV}$; $|\eta| < 2$; $p_T^l \geq 20 \text{ GeV}$
- LO distribution bounded at $m_T = 50 \text{ GeV}$. Around the bound there are perturbative instabilities from LO to NLO and to NNLO (Sudakov shoulder [Catani, Webber ('97)]).
- Below the boundary, the $\mathcal{O}(\alpha_S^2)$ corrections are large (e.g. +40% at $m_T \sim 30 \text{ GeV}$). Not unexpected: in this region the $\mathcal{O}(\alpha_S^2)$ result is only a NLO calculation.
- Accepted cross sections (errors refer to Monte Carlo numerical errors):
 - $\sigma_{LO} = 1.61 \pm 0.001 \text{ nb}$
 - $\sigma_{NLO} = 1.550 \pm 0.001 \text{ nb}$
 - $\sigma_{NNLO} = 1.586 \pm 0.002 \text{ nb}$
- σ_{NNLO} scales variation:
 - 0.8% for $\mu_R = \mu_F = m_W/2$,
 - +0.6% for $\mu_R = \mu_F = 2 m_W$.

Transverse mass distribution

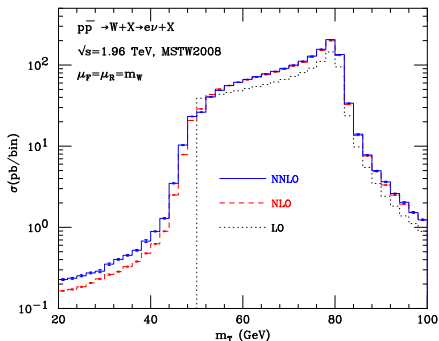


Transverse mass distribution for W production at the Tevatron:

$$m_T = \sqrt{2p_T^l p_T^{miss} (1 - \cos \phi_{l\nu})}$$

- Cuts: $p_T^{miss} \geq 25 \text{ GeV}$; $|\eta| < 2$; $p_T^l \geq 20 \text{ GeV}$
- LO distribution bounded at $m_T = 50 \text{ GeV}$. Around the bound there are perturbative instabilities from LO to NLO and to NNLO (Sudakov shoulder [Catani, Webber ('97)]).
- Below the boundary, the $\mathcal{O}(\alpha_S^2)$ corrections are large (e.g. +40% at $m_T \sim 30 \text{ GeV}$). Not unexpected: in this region the $\mathcal{O}(\alpha_S^2)$ result is only a NLO calculation.
- Accepted cross sections (errors refer to Monte Carlo numerical errors):
 - $\sigma_{LO} = 1.61 \pm 0.001 \text{ nb}$
 - $\sigma_{NLO} = 1.550 \pm 0.001 \text{ nb}$
 - $\sigma_{NNLO} = 1.586 \pm 0.002 \text{ nb}$
- σ_{NNLO} scales variation:
 - 0.8% for $\mu_R = \mu_F = m_W/2$,
 - +0.6% for $\mu_R = \mu_F = 2 m_W$.

Transverse mass distribution

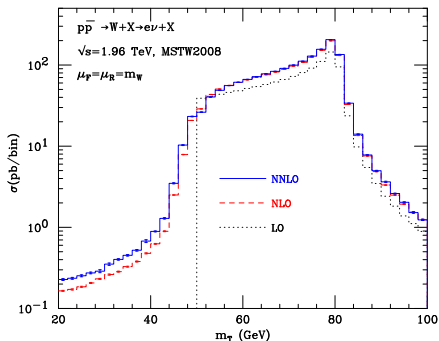


Transverse mass distribution for W production at the Tevatron:

$$m_T = \sqrt{2p_T^l p_T^{\text{miss}} (1 - \cos \phi_{l\nu})}$$

- Cuts: $p_T^{\text{miss}} \geq 25 \text{ GeV}$; $|\eta| < 2$; $p_T^l \geq 20 \text{ GeV}$
- LO distribution bounded at $m_T = 50 \text{ GeV}$. Around the bound there are perturbative instabilities from LO to NLO and to NNLO (Sudakov shoulder [Catani, Webber('97)]).
- Below the boundary, the $\mathcal{O}(\alpha_S^2)$ corrections are large (e.g. +40% at $m_T \sim 30 \text{ GeV}$). Not unexpected: in this region the $\mathcal{O}(\alpha_S^2)$ result is only a NLO calculation.
- Accepted cross sections (errors refer to Monte Carlo numerical errors):
 - $\sigma_{LO} = 1.61 \pm 0.001 \text{ nb}$
 - $\sigma_{NLO} = 1.550 \pm 0.001 \text{ nb}$
 - $\sigma_{NNLO} = 1.586 \pm 0.002 \text{ nb}$
- σ_{NNLO} scales variation:
 - 0.8% for $\mu_R = \mu_F = m_W/2$,
 - +0.6% for $\mu_R = \mu_F = 2 m_W$.

Transverse mass distribution



Transverse mass distribution for W production at the Tevatron:

$$m_T = \sqrt{2p_T^l p_T^{miss} (1 - \cos \phi_{l\nu})}$$

- Cuts: $p_T^{miss} \geq 25 \text{ GeV}$; $|\eta| < 2$; $p_T^l \geq 20 \text{ GeV}$
- LO distribution bounded at $m_T = 50 \text{ GeV}$. Around the bound there are perturbative instabilities from LO to NLO and to NNLO (Sudakov shoulder [Catani, Webber ('97)]).
- Below the boundary, the $\mathcal{O}(\alpha_S^2)$ corrections are large (e.g. +40% at $m_T \sim 30 \text{ GeV}$). Not unexpected: in this region the $\mathcal{O}(\alpha_S^2)$ result is only a NLO calculation.
- Accepted cross sections (errors refer to Monte Carlo numerical errors):
 $\sigma_{LO} = 1.61 \pm 0.001 \text{ nb}$
 $\sigma_{NLO} = 1.550 \pm 0.001 \text{ nb}$
 $\sigma_{NNLO} = 1.586 \pm 0.002 \text{ nb}$
- σ_{NNLO} scales variation:
 -0.8% for $\mu_R = \mu_F = m_W/2$,
 $+0.6\%$ for $\mu_R = \mu_F = 2 m_W$.

Conclusions

- We have presented a fully exclusive NNLO QCD calculation for vector boson production in hadron collisions [Catani, Cieri, G.F., de Florian, Grazzini: [arXiv:0903.2120]], based on the q_T subtraction formalism [Catani, Grazzini('07)].
- We have implemented the calculation in the parton level Monte Carlo code **DYNNLO**. The program allows the user to apply arbitrary kinematical cuts on the final state and on the associated jet activity computing the required distributions in the form of bin histograms.
- We have shown some illustrative numerical results for the Tevatron and the LHC.
- A public version of the numerical code **DYNNLO** is available at:
<http://theory.fi.infn.it/grazzini/dy.html>
- If you use this program please quote:
S. Catani, L. Cieri, G. Ferrera, D. de Florian and M. Grazzini, Phys. Rev. Lett. **103** (2009) 082001;
S. Catani and M. Grazzini, Phys. Rev. Lett. **98** (2007) 222002.

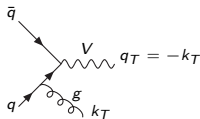
Back up slides

The q_T subtraction formalism

$$h_1(p_1) + h_2(p_2) \rightarrow V(M, q_T) + X$$

V is one or more **colourless** particles (vector bosons, leptons, photons, Higgs bosons, ...) [Catani, Grazzini('07)].

- **Key point I:** at LO the q_T of the V is exactly zero.



$$d\sigma_{(N)NLO}^V|_{q_T \neq 0} = d\sigma_{(N)LO}^{V+\text{jets}},$$

for $q_T \neq 0$ the NNLO IR divergences cancelled with the NLO subtraction method.

- The only remaining NNLO singularities are associated with the $q_T \rightarrow 0$ limit.
- **Key point II:** treat the NNLO singularities at $q_T = 0$ by an additional subtraction using the universality of logarithmically-enhanced contributions from q_T resummation formalism [Catani, de Florian, Grazzini('00)].

$$d\sigma_{N^n LO}^V \xrightarrow{q_T \rightarrow 0} d\sigma_{LO}^V \otimes \Sigma(q_T/M) dq_T^2 = d\sigma_{LO}^V \otimes \sum_{n=1}^{\infty} \sum_{k=1}^{2n} \left(\frac{\alpha_S}{\pi}\right)^n \Sigma^{(n,k)} \frac{M^2}{q_T^2} \ln^{k-1} \frac{M^2}{q_T^2} d^2 q_T$$

$$d\sigma^{CT} \xrightarrow{q_T \rightarrow 0} d\sigma_{LO}^V \otimes \Sigma(q_T/M) dq_T^2$$

The final result is:

$$d\sigma_{(N)NLO}^V = \mathcal{H}_{(N)NLO}^V \otimes d\sigma_{LO}^V + \left[d\sigma_{(N)LO}^{V+jets} - d\sigma_{(N)LO}^{CT} \right],$$

$$\text{where } \mathcal{H}_{NNLO}^V = \left[1 + \frac{\alpha_S}{\pi} \mathcal{H}^{V(1)} + \left(\frac{\alpha_S}{\pi} \right)^2 \mathcal{H}^{V(2)} \right]$$

- The choice of the counter-term has some arbitrariness but it must behave $d\sigma^{CT} \xrightarrow{q_T \rightarrow 0} d\sigma_{LO}^V \otimes \Sigma(q_T/M) dq_T^2$. Note that $\Sigma(q_T/M)$ is universal.
- $d\sigma^{CT}$ regularizes the $q_T = 0$ singularity of $d\sigma^{V+jets}$: *double real* and *real-virtual* NNLO contributions, while *two-loops virtual* correction are contained in \mathcal{H}_{NNLO}^V .
- Final state partons only appear in $d\sigma^{V+jets}$ so that NNLO IR cuts are included in the NLO computation: observable-independent NNLO extension of the subtraction formalism.
- NLO calculation requires $d\sigma_{LO}^{V+jets}$ and $\mathcal{H}^{V(1)}$ [de Florian, Grazzini('01)].
- At NNLO we need also $d\sigma_{NLO}^{V+jets}$ [Giele et al.('93), MCFM] and $\mathcal{H}^{V(2)}$.

- The general relation between $\mathcal{H}^{V(2)}$ and the IR finite part of the two-loops correction to a generic process is unknown. We explicit computed it for the DY process with the following method.

$$\sigma_{NNLO}^{V,tot} = \int_0^\infty dq_T^2 \frac{d\sigma_{NLO}^V}{dq_T^2}.$$

- We decompose the q_T distribution as following:

$$\frac{d\sigma_{NLO}^V}{dq_T^2} = \frac{d\sigma_{NLO}^{V,(res.)}}{dq_T^2} + \frac{d\sigma_{NLO}^{V,(fin.)}}{dq_T^2},$$

where the first term on the r.h.s. contains all the the logarithmically-enhanced contributions at small q_T while the second term is free of such contributions.

- Following the [Bozzi, Catani, de Florian, Grazzini('06)] formalism we can then write

$$\sigma_{NNLO}^{V,tot} = \sigma_{LO}^V \mathcal{H}_{NNLO}^V + \int_0^\infty dq_T^2 \frac{d\sigma_{NLO}^{V,(fin.)}}{dq_T^2}.$$

- This formula allows us to analytically compute \mathcal{H}_{NNLO}^V from the knowledge of the NNLO total cross section and the NLO q_T distribution.